

pubs.acs.org/JPCB Article

Energy, Work, Entropy, and Heat Balance in Marcus Molecular Junctions

Published as part of The Journal of Physical Chemistry virtual special issue "Peter J. Rossky Festschrift". Natalya A. Zimbovskaya and Abraham Nitzan*



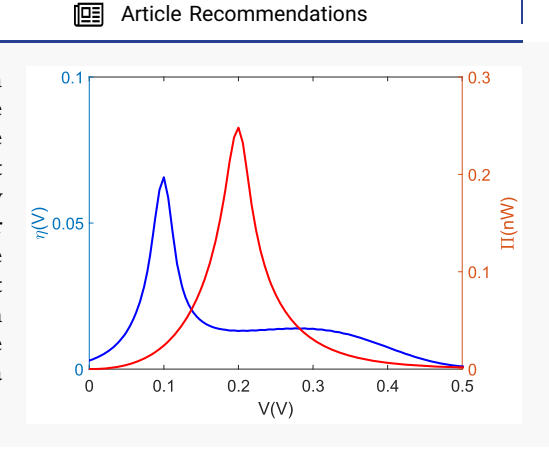
Cite This: J. Phys. Chem. B 2020, 124, 2632-2642



ACCESS

III Metrics & More

ABSTRACT: We present a consistent theory of energy balance and conversion in a single-molecule junction with strong interactions between electrons on the molecular linker (dot) and phonons in the nuclear environment where the Marcus-type electron hopping processes predominate in the electron transport. It is shown that the environmental reorganization and relaxation that accompany electron hopping energy exchange between the electrodes and the nuclear (molecular and solvent) environment may bring a moderate local cooling of the latter in biased systems. The effect of a periodically driven dot level on the heat transport and power generated in the system is analyzed, and energy conservation is demonstrated both within and beyond the quasistatic regime. Finally, a simple model of atomic scale engine based on a Marcus single-molecule junction with a driven electron level is suggested and discussed.



I. INTRODUCTION

In the past two decades molecular electronics became a wellestablished and quickly developing field. 1-5 Presently, it provides a general platform which can be used to consider diverse nanoscale electronic and energy conversion devices. The basic building block of such devices is a single-molecule junction (SMJ). This system consists of a couple of metallic/ semiconducting electrodes linked with a molecular bridge. Electron transport through SMJs is controlled by electric forces, thermal gradients, and electron-phonon interactions. In addition, in SMJs operating inside dielectric solvents, transport properties may be strongly affected by the solvent response to the molecule's charge states.⁶⁻⁸ Overall, electrons on the molecule may interact with a collection of thermalized phonon modes associated with the solvent nuclear environment as well as with individual modes associated with molecular vibrations. Such interactions lead to the energy exchange between traveling electrons and the environment, thus giving rise to inelastic effects in the electron transport. In the weak electron-phonon coupling limit, inelastic contributions may be treated as perturbations of basically elastic transport. 9-16 Stronger coupling of electrons to phonon modes can result in several interesting phenomena including negative differential conductance, rectification, and Franck-Condon blockade.17-22

In the present work, we consider a limit of very strong electron-phonon interactions when electron transport may be described as a sequence of hops between the electrodes and

the bridge sites and/or among the bridge sites subjected to local thermalization. This dynamics is usually described by successive Marcus-type electron transfer processes. 3,23-27 Indeed, Marcus theory has been repeatedly and successfully used to study charge transport through redox molecules. 28-35 Nuclear motions and reorganization are at the core of this transport mechanism. The theory may be modified to include effects of temperature gradients across an SMJ 36,37 as well as a finite relaxation time of the solvent environment. Further generalization of Marcus theory accounting for finite lifetime broadening of the molecule electron levels was recently suggested. 38,39

Besides charge transport, electron—phonon interactions may strongly affect heat generation and transport through SMJs. S,10,20 There is an increasing interest in studies of vibrational heat transport in atomic scale systems and in their interfaces with bulk substrates. Electron transfer induced heat transport was also suggested and analyzed. Effects of structure—transport correlations on heat transport characteristics of such systems are being studied as well as effects originating from specific features of coupling between the

Received: January 3, 2020 Revised: March 6, 2020 Published: March 12, 2020



molecular linker and electrodes^{49–52} and the heat currents rectification. S3–55 Correlations between structure and heat transfer in SMJs and similar systems may be accompanied by heating/cooling of the molecular bridge environment. 9,10,56–61

Nevertheless, the analysis of heat transfer in SMJs is far from being completed, especially in molecular junctions dominated by Marcus-type electron transfer processes. In the present work, we theoretically analyze energy balance and conversion in such systems. For the molecular bridge, we use the standard single-level model that describes two molecular electronic states in which the level is either occupied or unoccupied. The electrodes are treated as free electron reservoirs with respective chemical potentials and temperatures. We assume that the level may be slowly driven by an external agent (such as a gate voltage) which moves it over a certain energy range. Also, we assume that the temperature of the solvent environment of the bridge may differ from the electrode temperatures. Despite its simplicity, the adopted model captures essential physics of energy conversion in such a junction.

The paper is organized as follows. In Section II, we review the application of Marcus rates to the evaluation of steady state currents resulting from voltage and temperature bias across the junction. We study the relationship between heat currents flowing into the electrodes and into the solvent environment of the molecular bridge and demonstrate overall energy conservation. In Section III, we analyze the energy balance in a system where a bridge electronic level is driven by an external force. We discuss the irreversible work thus done on the system and the corresponding dissipated power and the entropy change. In Section IV, we describe a simple model for a Marcus junctione engine and estimate its efficiency. Our conclusions are given in Section V.

II. STEADY STATE CURRENTS

II.A. Electron Transfer Rates and Electronic Currents.

We consider a molecular junction where electrons move between electrodes through a molecular bridge (or dot) that can be occupied (state a) or unoccupied (state b). Adopting the Marcus formalism, we assume that each state corresponds to a free energy surface which is assumed to be parabolic in the collective solvent coordinate x. Here and below, we take "solvent" to include also the intramolecular nuclear motion which contributes to the electronic charge accumulation. We use the simplest shifted surfaces model: In terms of x, the energy surfaces associated with the two electronic states are assumed to take the forms of identical harmonic surfaces that are shifted relative to each other.

$$E_a(x) = \frac{1}{2}kx^2\tag{1}$$

$$E_b(x) = \frac{1}{2}k(x - \lambda)^2 + \epsilon_d$$
 (2)

Here, λ represents a shift in the equilibrium value of the reaction coordinate, and $\epsilon_{\rm d}$ is the difference between the equilibrium energies of the two electronic states. Diverse reaction geometries may be taken into account by varying $\epsilon_{\rm d}$ and the force constants. More sophisticated models make the mathematics more involved but are not expected to change the essential physics. The reorganization energy $E_{\rm r}$ associated with the electron transfer process

$$E_{\rm r} = \frac{1}{2}k\lambda^2\tag{3}$$

reflects the strength of interactions between electrons on the bridge and the solvent environment. For $E_{\rm r}=0$, electron transport becomes elastic.

The overall kinetic process is determined by the transfer rates $k_{a\to b}^{\mathrm{L,R}}$ and $k_{b\to a}^{\mathrm{L,R}}$ which correspond to transitions at the left (L) and right (R) electrodes between the occupied (a) and unoccupied (b) molecular states (namely, $a\to b$ corresponds to electron transfer from molecule to metal and $b\to a$ denotes the opposite process). Because of the time scale separation between electron and nuclear motions, these transfer processes have to satisfy electronic energy conservation:

$$g(x, \epsilon) = E_b(x) - E_a(x) + \epsilon = 0 \tag{4}$$

where ϵ is the energy of electron in the metal. This leads to the Marcus electron transfer rates given by 27

$$k_{a \to b}^{K} = \sqrt{\frac{\beta_{s}}{4\pi E_{r}}} \int_{-\infty}^{\infty} d\epsilon \, \Gamma_{K}(\epsilon) [1 - f_{K}(\beta_{K}, \epsilon)]$$

$$\times \exp\left[-\frac{\beta_{s}}{4E_{r}} (\epsilon + E_{r} - \epsilon_{d})^{2}\right]$$

$$k_{b \to a}^{K} = \sqrt{\frac{\beta_{s}}{4\pi E_{r}}} \int_{-\infty}^{\infty} d\epsilon \, \Gamma_{K}(\epsilon) f_{K}(\beta_{K}, \epsilon)$$

$$\times \exp\left[-\frac{\beta_{s}}{4E_{r}} (\epsilon_{d} + E_{r} - \epsilon)^{2}\right]$$
(6)

where $K = \{L, R\}$ stands for the left and right electrodes. In these expressions, $\Gamma_K = 2\pi V_K^2 \rho_K / \hbar$ where ρ_K is the single electron density of states for the electrode K and V_K the tunneling coupling for electron transfer between this electrode and the molecule. $\beta_{\rm L,R}=(kT_{\rm L,R})^{-1}$ and $\beta_{\rm s}=(kT_{\rm s})^{-1}$ indicate the temperatures of the electrodes and the molecule environment. k is the Boltzmann constant, and $f_{\rm L,R}$ are Fermi distribution functions for the electrodes with chemical potentials $\mu_{L,R}$. Expressions in eqs 5 and 6 assume that electron transfer takes place from an equilibrium solvent and metal configurations, namely, that thermal relaxation in the metal and solvent environments are fast relative to the metalmolecule electron exchange processes. When $T_L = T_R = T_{s'}$ eqs 5 and 6 are reduced to the standard Marcus-Hush-Chidsey expressions for electron-electrode transfer rates. 27,62 In further analysis, we assume that the molecule is symmetrically coupled to the electrodes ($\Gamma_{\rm L}$ = $\Gamma_{\rm R}$ = Γ), and unless stated otherwise, we take Γ as a constant independent of energy.

Given these rates, the probabilities that the dot is in the states a or b at time t, P_a and P_b , are determined by the kinetic equations

$$\frac{\mathrm{d}P_a}{\mathrm{d}t} = P_b k_{b \to a} - P_a k_{a \to b} \qquad \frac{\mathrm{d}P_b}{\mathrm{d}t} = P_a k_{a \to b} - P_b k_{b \to a} \tag{7}$$

where $k_{a \to b} = k_{a \to b}^{\rm L} + k_{a \to b}^{\rm R}$; $k_{b \to a} = k_{b \to a}^{\rm L} + k_{b \to a}^{\rm R}$. The steady state probabilities P_a^0 and P_b^0 and the steady state electron current $I_{\rm ss}$ (positive when electrons go from left to right) are given by

$$P_a^0 = \frac{k_{b \to a}}{k_{a \to b} + k_{b \to a}} \qquad P_b^0 = \frac{k_{a \to b}}{k_{a \to b} + k_{b \to a}}$$
(8)

$$\frac{I_{ss}}{|e|} = k_{b\to a}^{L} P_{b}^{0} - k_{a\to b}^{L} P_{a}^{0}
= -(k_{b\to a}^{R} P_{b}^{0} - k_{a\to b}^{R} P_{a}^{0})
= \frac{k_{a\to b}^{R} k_{b\to a}^{L} - k_{b\to a}^{R} k_{a\to b}^{L}}{(k_{a\to b} + k_{b\to a})}$$
(9)

The coupling Γ of the molecular bridge to electrodes affects the electron transfer rates (and consequently the SMJ transport properties) in two ways. First, as indicated above, it controls the transfer rates between the electrodes and the molecule. This effect is accounted for within the standard Marcus theory. Second, it is manifested in the lifetime broadening of molecular levels, an effect disregarded by this theory. It has been suggested in recent work that the Marcus expressions for the transfer rates may be generalized to include the broadening effect. For a symmetrically coupled system the transfer rates may be approximated as follows: 38,39

$$k_{a\to b}^{\rm L,R} = \frac{\Gamma}{\pi} \int_{-\infty}^{\infty} \, {\rm d}\epsilon \, [1 - f_{\rm L,R}(\beta_{\rm L,R},\,\epsilon)] K_-(\epsilon) \eqno(10)$$

$$k_{b\to a}^{\rm L,R} = \frac{\Gamma}{\pi} \int_{-\infty}^{\infty} \, \mathrm{d}\epsilon f_{\rm L,R}(\beta_{\rm L,R},\epsilon) K_{+}(\epsilon) \tag{11}$$

where

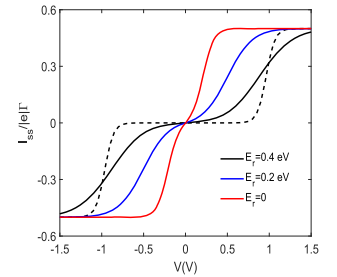
$$K_{\pm}(\epsilon) = Re \left[\sqrt{\frac{\pi \beta_s}{4E_r}} \exp \left[-\frac{\beta_s}{4E_r} (\hbar \Gamma \mp i(\epsilon_d \pm E_r - \epsilon))^2 \right] \right]$$

$$\times \operatorname{erfc} \left[\sqrt{\frac{\beta_s}{4E_r}} (\hbar \Gamma \mp i(\epsilon_d \pm E_r - \epsilon)) \right]$$
(12)

and erfc(x) is the complementary error function. Although the derivation of eqs 10-12 involves some fairy strong assumptions, 38,39 the result is attractive for its ability to yield the Landauer cotunneling expression in the strong moleculeelectrode coupling limit $\sqrt{E_r k T_s} \ll \hbar \Gamma$ and the Marcus expression in the opposite limit. This is shown in the left panel of Figure 1 where three current-voltage curves are plotted at the same value of Γ and several values of E_r . The Landauer-Buttiker behavior is demonstrated for $E_r = 0$. As E_r enhances, the current-voltage curve behavior becomes more similar to the Marcus behavior represented by the dashed line. In the case of the Marcus limit, one observes a very pronounced plateau in the I-V profile around V=0, as seen in Figure 1 (dashed line). This plateau develops gradually as the electron-phonon coupling increases and is a manifestation of a Franck-Condon blockade similar to that resulting from interactions between electrons and individual molecular vibrational modes. 19,20

When the two electrodes in an unbiased SMJ ($\mu_{\rm L}=\mu_{\rm R}=\mu$) are kept at different temperatures, a thermally induced charge current emerges, as shown in Figure 1 (right panel). The current does not appear if $\epsilon_{\rm d}=\mu=0.^{66}$ However, when $\epsilon_{\rm d}\neq\mu$ the current emerges. The current changes its direction at $T_{\rm L}=T_{\rm R}$. Its magnitude strongly depends on the reorganization energy. Indeed, the thermally induced current takes on noticeable values only provided that the effects of nuclear reorganization are weak and becomes suppressed when the interaction with the solvent environment increases.

II.B. Heat Currents and Energy Conservation. The results summarized above were mostly obtained before in



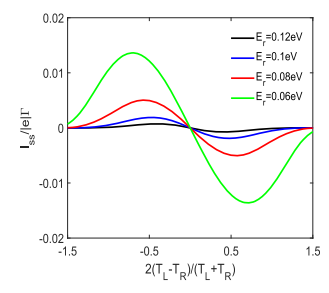


Figure 1. Left panel: Current—voltage characteristics computed using eqs 10–12 (solid lines). The electrode Fermi energy in the unbiased junction is set to 0; the bias is applied symmetrically ($\mu_{\rm L,R}=\pm {\rm lel}V/2$) relative to this origin and $T_{\rm L}=T_{\rm R}=T_{\rm s}$. The Landauer—Buttiker limit is represented by the red line ($E_{\rm r}=0$). The difference between the results obtained using eqs 10–12 and the Marcus limit is demonstrated by comparison of the solid black line with the dashed line plotted using the Marcus equations for the electron transfer rates at the same value of $E_{\rm r}$ ($E_{\rm r}=0.4$ eV). Right panel: Electron current as a function of the temperature difference symmetrically distributed between the electrodes (($T_{\rm L}+T_{\rm R})/2=T_{\rm s}$) in an unbiased SMJ in the Marcus limit. Curves are plotted assuming that $kT_{\rm s}=0.026$ eV, $\hbar\Gamma=0.01$ eV, $\epsilon_{\rm d}=0.1$ eV (left panel), and $\epsilon_{\rm d}=-0.02$ eV (right panel).

works that investigate the implication of Marcus kinetics for the steady state conduction properties of molecular junctions in the limit of hopping conduction. Here we focus on the energy balance associated with such processes, and the implication of Marcus kinetics on heat transfer. Each electron hopping event between the molecule and an electrode is accompanied by solvent and metal relaxation and, therefore, by heat production in these environments. We denote these heats Q_s and Q_e for the solvent and the electrode, respectively. Specifically, $Q_{s,a\rightarrow b}^{L,R}$ denotes the heat change in the solvent when an electron hops from the molecule into the left (L) or right (R) electrode, and similarly, $Q_{s,b\rightarrow a}^{L,R}$ is heat change in the solvent in the opposite process of an electron moving from the electrode to the molecule. For symmetrically coupled electrodes ($\Gamma_L = \Gamma_R = \Gamma$) considered in the Marcus limit, these terms have the form

$$Q_{s,a\to b}^{K} = \frac{\Gamma}{k_{a\to b}^{K}} \sqrt{\frac{\beta_{s}}{4\pi E_{r}}} \int d\epsilon [1 - f_{K}(\beta_{K}, \epsilon)] (\epsilon_{d} - \epsilon)$$

$$\times \exp \left[-\frac{\beta_{s}}{4E_{R}} (E_{r} - \epsilon_{d} + \epsilon)^{2} \right]$$
(13)

and

$$Q_{s,b\to a}^{K} = \frac{\Gamma}{k_{b\to a}^{K}} \sqrt{\frac{\beta_{s}}{4\pi E_{r}}} \int d\epsilon f_{K}(\beta_{K}, \epsilon)(\epsilon - \epsilon_{d})$$

$$\times \exp\left[-\frac{\beta_{s}}{4E_{R}}(\epsilon_{d} + E_{r} - \epsilon)^{2}\right]$$
(14)

where $K = \{L, R\}$. Similarly, $Q_{e,a \to b}^K$ and $Q_{e,b \to a}^K$ are heats generated in electrode K when an electron leaves (enters) the molecule into (from) that electrode:

$$Q_{e,a\to b}^{K} = \frac{\Gamma}{k_{a\to b}^{K}} \sqrt{\frac{\beta_{s}}{4\pi E_{r}}} \int d\epsilon [1 - f_{K}(\beta_{K}, \epsilon)](\epsilon - \mu_{K})$$

$$\times \exp\left[-\frac{\beta_{s}}{4E_{r}}(E_{r} - \epsilon_{d} + \epsilon)^{2}\right]$$
(15)

and

$$Q_{e,b\to a}^{K} = \frac{\Gamma}{k_{b\to a}^{K}} \sqrt{\frac{\beta_{s}}{4\pi E_{r}}} \int d\epsilon f_{K}(\beta_{K}, \epsilon) (\mu_{K} - \epsilon)$$

$$\times \exp\left[-\frac{\beta_{s}}{4E_{R}} (\epsilon_{d} + E_{r} - \epsilon)^{2}\right]$$
(16)

Equations 15 and 16 are analogues of the corresponding results reported in ref 37.

Equations 13–16 are expressions for the heat changes per specific hopping events. The corresponding heat change rates (heat per unit time) in the solvent and the electrodes are obtained from

$$J_{s} \equiv \dot{Q}_{s}$$

$$= P_{a}^{0} (k_{a \to b}^{L} Q_{s,a \to b}^{L} + k_{a \to b}^{R} Q_{s,a \to b}^{R})$$

$$+ P_{b}^{0} (k_{b \to a}^{L} Q_{s,b \to a}^{L} + k_{b \to a}^{R} Q_{s,b \to a}^{R})$$
(17)

and

$$J_{e}^{K} \equiv \dot{Q}_{e}^{K} = k_{a \to b}^{K} P_{a}^{0} Q_{e,a \to b}^{K} + k_{b \to a}^{K} P_{b}^{0} Q_{e,b \to a}^{K}$$
(18)

Using eqs 5 and 6 and eqs 13–16, it can be easily established that eqs 17 and 18 imply

$$J_{e}^{L} + J_{e}^{R} + J_{s} = (\mu_{L} - \mu_{R})I_{ss}$$
 (19)

showing the balance between heat change rates in the solvent and the electrodes and the heat generated by the current flow across the voltage bias. In the absence of solvent reorganization, $J_s=0$ and eq 19 is reduced to the standard junction energy balance relation $J_{\rm e}^{\rm L}+J_{\rm e}^{\rm R}=(\mu_{\rm L}-\mu_{\rm R})I_{\rm ss}/|{\rm el}|$. From eqs 13–18 we obtain after some algebra (see Appendix A)

$$J_{\rm e}^{\rm L} = (\mu_{\rm L} - \epsilon_{\rm d})I_{\rm ss} - (P_a^0 k_{a \to b}^{\rm L} + P_b^0 k_{b \to a}^{\rm L})E_{\rm r} - Y_{\rm L}$$
 (20)

$$J_{\rm e}^{\rm R} = (\epsilon_{\rm d} - \mu_{\rm R})I_{\rm ss} - (P_a^0 k_{a \to b}^{\rm R} + P_b^0 k_{b \to a}^{\rm R})E_{\rm r} - Y_{\rm R}$$
 (21)

$$J_{s} = 2 \frac{k_{a \to b} k_{b \to a}}{k_{a \to b} + k_{b \to a}} E_{r} + Y_{L} + Y_{R}$$
(22)

where

$$Y_{K} = \Gamma \sqrt{\frac{E_{r}}{\pi \beta_{s}}} \int d\varepsilon \frac{\partial f_{K}}{\partial \varepsilon}$$

$$\times \left[P_{b}^{0} \exp \left[-\frac{\beta_{s}}{4E_{R}} (\varepsilon_{d} + E_{r} - \varepsilon)^{2} \right] + P_{a}^{0} \exp \left[-\frac{\beta_{s}}{4E_{R}} (E_{r} - \varepsilon_{d} + \varepsilon)^{2} \right] \right]$$
(23)

The analysis presented in this section remains valid regardless of the specific form of the expressions for the relevant heat flows. These may be defined within Marcus theory by eqs 13–16 or by the generalized expressions derived using the approximation of ref 38:

$$Q_{s,a\to b}^{L,R} = \frac{1}{\pi} \frac{\Gamma}{k_{a\to b}^{L,R}} \int d\epsilon [1 - f_{L,R}(\beta_{L,R}, \epsilon)] (\epsilon_{d} - \epsilon) K_{-}(\epsilon)$$
(24)

$$Q_{s,b\rightarrow a}^{L,R} = \frac{1}{\pi} \frac{\Gamma}{k_{b\rightarrow a}^{L,R}} \int d\epsilon f_{L,R}(\beta_{L,R}, \epsilon) (\epsilon - \epsilon_{\rm d}) K_{+}(\epsilon)$$
 (25)

$$\begin{split} Q_{\mathrm{e},a\to b}^{\mathrm{L,R}} &= \frac{1}{\pi} \frac{\Gamma}{k_{a\to b}^{\mathrm{L,R}}} \int \, \mathrm{d} \epsilon [1 - f_{\mathrm{L,R}}(\beta_{\mathrm{L,R}},\, \epsilon)] (\epsilon - \mu_{\mathrm{L,R}}) \\ &\quad K_{-}(\epsilon) \end{split} \label{eq:epsilon}$$
 (26)

$$Q_{e,b\to a}^{L,R} = \frac{1}{\pi} \frac{\Gamma}{k_{b\to a}^{L,R}} \int d\epsilon f_{L,R}(\beta_{L,R}, \epsilon) (\mu_{L,R} - \epsilon) K_{+}(\epsilon)$$
(27)

where $k_{a\to b}^{\rm L,R}$, $k_{b\to a}^{\rm L,R}$, and $K_{\pm}(\epsilon)$ are given by eqs 10–12. It should be noted that the procedure leading to eq 19 that demonstrates the energy conservation remains the same when these expressions are used.

Results based on eqs 20-23 obtained using Marcus theory rates given by eqs 5 and 6 are displayed in Figure 2. The left

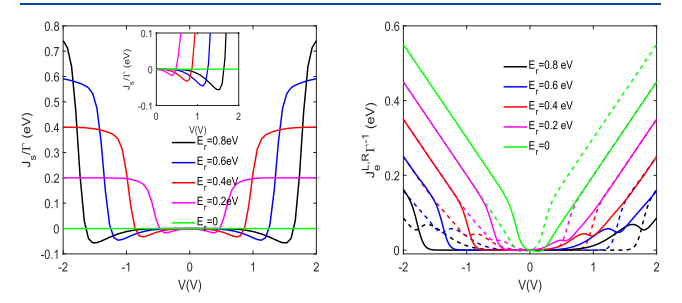


Figure 2. Heat currents J_s (left panel), $J_{\rm e}^{\rm L}$ (solid lines, right panel), and $J_{\rm e}^{\rm R}$ (dashed lines, right panel) shown as functions of the bias voltage V for several values of the reorganization energy. Curves are plotted omitting the effect of molecular level broadening and assuming $kT_s = kT_{\rm L} = kT_{\rm R} = 0.026$ eV, $\hbar\Gamma = 0.01$ eV, $\epsilon_{\rm d} = 0.1$ eV. The inset in the left panel focuses on a segment of the main plot that emphasizes the local cooling of the solvent in the corresponding voltage range.

panel shows the heat deposited in the solvent environment plotted against the bias voltage for different values of the reorganization energy. The right panel shows similar results for the left and right electrodes. The following observations can be made:

- (a) Reflecting the behavior of the electronic current, energy exchange processes are very weak at low bias due to the Franck—Condon blockade that hinders electron transport. Noticeable heat currents appear when lelV exceeds the reorganization energy E_r thus lifting the blockade.
- (b) The heat deposited into the electrodes shows an asymmetry between positive and negative biases (or equivalently between left and right electrodes). This asymmetry reflects the different positioning of the energy of the transferred electron relative to the left and right Fermi energies⁶⁵ and was observed experimentally.⁶⁷
- (c) The heat deposited into the solvent environment (left panel) is symmetric with respect to bias inversion because it reflects the energy balance relative to both electrodes.
- (d) Note that the heat exchanged with the solvent (nuclear) environment can become negative; namely, heat may be pulled out of this environment at some range of bias and reorganization energy. In the present case of a symmetrically coupled SMJ with a symmetrically distributed bias voltage, this happens at $|eV| \approx 2E_{r}$,

namely, when the driving force associated with the bias voltage is nearly counterbalanced by driving for the solvent reorganization originated from electron—phonon interactions. This cooling is reminiscent of similar effects discussed in the low electron—phonon coupling regime. $^{59-61}$

III. DRIVEN JUNCTION

Next we consider charge and energy currents in driven biased junctions, where driving is modeled by an externally controlled time dependent parameter in the system Hamiltonian. In the present study we limit our consideration to time dependence of the single electron "level" $\epsilon_{\rm d}$ of the molecular bridge that may in principle be achieved by varying the gate potential. Similar studies in the absence of electron—phonon interactions, focusing on a consistent quantum thermodynamic description of such systems, were recently published. The model considered below includes strong coupling to the phonon environment at the cost of treating this coupling semiclassically and assuming weak coupling between the molecule and the electrodes. This model is similar to that used to analyze cyclic voltammetry observations when extended to consider two metal interfaces.

In further analysis we assume that the electron level $\epsilon_{\rm d}$ is a slowly varying and construct an expansion of the solution of in powers of $\dot{\epsilon}_{\rm d}$. To this end we start by separating the time dependent populations into their steady state components (which implicitly depend on time through $\epsilon_{\rm d}(t)$) and corrections defined by 29

$$P_a(t) = P_a^0(\epsilon_d) - G(\epsilon_d, t)$$

$$P_b(t) = P_b^0(\epsilon_d) + G(\epsilon_d, t)$$
(28)

where the steady state populations $P_{a,b}^0$ satisfy $P_b k_{b \to a} - P_a k_{a \to b} = 0$, $P_a + P_b = 1$, and are given by eq 8. Then

$$\frac{\mathrm{d}P_a}{\mathrm{d}t} = \dot{\varepsilon}_\mathrm{d} \frac{\partial P_a^0}{\partial \varepsilon_\mathrm{d}} - \frac{\mathrm{d}G}{\mathrm{d}t}$$

$$\frac{\mathrm{d}P_b}{\mathrm{d}t} = \dot{\epsilon}_{\mathrm{d}} \frac{\partial P_b^0}{\partial \epsilon_{\mathrm{d}}} + \frac{\mathrm{d}G}{\mathrm{d}t} \tag{29}$$

From eqs 28 it follows that

$$\frac{\mathrm{d}P_a}{\mathrm{d}t} = -\frac{\mathrm{d}P_b}{\mathrm{d}t} = G(k_{a\to b} + k_{b\to a}) \tag{30}$$

Comparing eqs 29 and 30, we obtain

$$\frac{\mathrm{d}G}{\mathrm{d}t} = \dot{\epsilon}_{\mathrm{d}} \frac{\partial P_a^0}{\partial \epsilon_d} - G(k_{a \to b} + k_{b \to a}) \tag{31}$$

The electronic currents can be written in terms of G in the form

$$I_{L} = k_{b \to a}^{L} P_{b} - k_{a \to b}^{L} P_{a} = I_{ss} + I_{L}^{excess}$$

$$I_{R} = k_{b \to a}^{R} P_{b} - k_{a \to b}^{R} P_{a} = I_{ss} + I_{R}^{excess}$$
(32)

(where $I_K^{\text{excess}} = (k_{b \to a}^K + k_{a \to b}^K)G$) expressing the fact that the left and right excess particle (electron) currents due to driving are generally not the same. Equations 32 together with analogues of eqs 17 and 18 in which $P_{a,b}^0$ are replaced by $P_{a,b}$ which can be used to obtain the excess heat currents caused by driving

$$J_{s}^{\text{excess}} = \dot{Q}_{s}^{\text{excess}}$$

$$= G(k_{b \to a}^{\text{L}} Q_{s,b \to a}^{\text{L}} - k_{a \to b}^{\text{L}} Q_{s,a \to b}^{\text{L}}$$

$$+ k_{b \to a}^{\text{R}} Q_{s,b \to a}^{\text{R}} - k_{a \to b}^{\text{R}} Q_{s,a \to b}^{\text{R}})$$
(33)

$$J_{e}^{K,\text{excess}} = \dot{Q}_{e}^{K,\text{excess}} = G(k_{b \to a}^{K} Q_{e,b \to a}^{K} - k_{a \to b}^{K} Q_{e,a \to b}^{K})$$
(34)

Using these expressions with eqs 13-16 for the heat currents and eqs 5 and 6, or 10 and 11, we find

$$J_{\text{tot}}^{\text{excess}} \equiv J_{\text{s}}^{\text{excess}} + J_{\text{e}}^{\text{L,excess}} + J_{\text{e}}^{\text{R,excess}}$$

$$= G[(\mu_{\text{L}} - \epsilon_{\text{d}})(k_{a \to b}^{\text{L}} + k_{b \to a}^{\text{L}})$$

$$+ (\mu_{\text{R}} - \epsilon_{\text{d}})(k_{a \to b}^{\text{R}} + k_{b \to a}^{\text{R}})]$$
(35)

Equations 31–35 are exact relations. In particular, eq 31 can be used as a basis for expansions in powers of $\dot{\varepsilon}_{\rm d}$. We start by writing G as such a power series, $G = G^{(1)} + G^{(2)} + ...$ with $G^{(n)}$ representing order n in $\dot{\varepsilon}_{\rm d}$, and use this expansion in eq 31 while further assuming that G depends on time only through its dependence on $\varepsilon_{\rm d}$. Therefore, ${\rm d}G^{(n)}/{\rm d}t$ is of the order n+1. We note that our results are consistent with this assumption.

III.A. Quasistatic Limit: First Order Corrections. To the first order in $\dot{\epsilon}_d$, the left-hand side of eq 31 vanishes, leading to

$$G^{(1)} = \dot{\mathbf{e}}_{\mathbf{d}} \frac{\partial P_a^0}{\partial \mathbf{e}_{\mathbf{d}}} \frac{1}{(k_{a \to b} + k_{b \to a})}$$
(36)

where $k_{a \to b}$ and $k_{b \to a}$ depend on time through their dependence on $\epsilon_{\rm d}$. Note that eqs 30 and 36 imply that ${\rm d}P_a^{(1)}/{\rm d}t = -{\rm d}P_b^{(1)}/{\rm d}t = \dot{\epsilon}_d\partial P_a^0/\partial \epsilon_{\rm d}$; namely, this order of the calculation corresponds to the quasistatic limit where all dynamics is derived from the time dependence of $\epsilon_{\rm d}$. At the same time, it should be emphasized that this limit is not a reflection of the instantaneous steady state, as is evident from eqs 32.

Consider first the electronic current. Using eqs 32 and 36, the first order correction to the electron exchange rates with the left and right electrodes is obtained in the form

$$I_K^{(1)} = (k_{b \to a}^K + k_{a \to b}^K) G^{(1)} = \dot{\epsilon}_{d} \frac{\partial P_a^0}{\partial \epsilon_{d}} \nu_K$$
(37)

with

$$\nu_K = \frac{k_{a \to b}^K + k_{b \to a}^K}{k_{a \to b} + k_{b \to a}} \tag{38}$$

namely, a product of the (first order) change in the electronic population on the molecule $\mathrm{d}P_a^{(1)}/\mathrm{d}t$ and the fraction ν_K of this change associated with the electrode K.

Next, consider the heat currents. Using eq 36 for G in eq 35 leads to

$$J_{\text{tot}}^{(1)} = -\epsilon_{\text{d}} \dot{\epsilon}_{\text{d}} \frac{\partial P_{a}^{0}}{\partial \epsilon_{\text{d}}} + \dot{\epsilon}_{\text{d}} \frac{\partial P_{a}^{0}}{\partial \epsilon_{\text{d}}} (\mu_{\text{L}} \nu_{\text{L}} + \mu_{\text{R}} \nu_{\text{R}})$$
(39)

To better elucidate the physical meaning of this result we rearrange the first term on the right according to $-\epsilon_{\rm d}\dot{\epsilon}_{\rm d}\partial P_a^0/\partial\epsilon_{\rm d}=\dot{\epsilon}_{\rm d}P_a^0-{\rm d}(\epsilon_d P_a^0)/{\rm d}t$ and use eq 37 to cast eq 39 in the form

$$\frac{\mathrm{d}(\epsilon_{\rm d} P_a^0)}{\mathrm{d}t} \equiv \dot{E}_{\rm M}^{(1)} = \dot{\epsilon}_{\rm d} P_a^0 - J_{\rm tot}^{(1)} + \mu_{\rm L} \dot{n}_{\rm L} + \mu_{\rm R} \dot{n}_{\rm R} \tag{40}$$

This equation is a statement of the first law of thermodynamics, where $\dot{E}_{\rm M}^{(1)}$ represents, to order 1, the rate of change of energy in the molecule, and the terms on the right stand for the work per unit time $(\dot{\epsilon}_d P_a^0)$, rate of heat developing in the environment $(-J_{\rm tot}^{(1)} \equiv -(J_{\rm e}^{\rm L(1)} + J_{\rm e}^{\rm R(1)} + J_{\rm s}^{(1)}))$, and rate of chemical work $(\mu_{\rm L} J_{\rm L}^{(1)} + \mu_{\rm R} J_{\rm R}^{(1)})$ to the same order. All terms included in eq 40 are of the form $\dot{\epsilon}_d r(\epsilon_d)$ where r is an arbitrary function and are therefore the same except of sign when ϵ_d goes up or down, as this should be within the quasistatic regime.

III.B. Beyond the Quasistatic Regime: Second Order Corrections. Using the expansion for G in eq 31 and keeping only second order terms leads to

$$G^{(2)} = -\frac{1}{k_{a \to b} + k_{b \to a}} \frac{\mathrm{d}G^{(1)}}{\mathrm{d}t}$$
(41)

which, using eq 36, gives

$$G^{(2)} = -\frac{\dot{\epsilon}_{d}^{2}}{(k_{a\rightarrow b} + k_{b\rightarrow a})} \frac{\partial}{\partial \epsilon_{d}} \left[\frac{\partial P_{a}^{0}}{\partial \epsilon_{d}} \frac{1}{(k_{a\rightarrow b} + k_{b\rightarrow a})} \right]$$
(42)

The second order correction to the electron current is $(K = \{L, R\})$:

$$I_K^{(2)} = (k_{a \to b}^K + k_{b \to a}^K) G^{(2)}$$

$$= -\dot{\epsilon}_d^2 \frac{\partial}{\partial \epsilon_d} \left[\frac{\partial P_a^0}{\partial \epsilon_d} \frac{1}{(k_{a \to b} + k_{b \to a})} \right] \nu_K$$
(43)

The second order excess heat is obtained from eq 35 by replacing G with $G^{(2)}$. The sum of second order corrections to the heat currents then takes the form

$$\begin{split} J_{\text{tot}}^{(2)} &\equiv J_{\text{e}}^{\text{L}(2)} + J_{\text{e}}^{\text{R}(2)} + J_{\text{s}}^{(2)} \\ &= -\epsilon_{\text{d}} G^{(2)} (k_{a \to b} + k_{b \to a}) + G^{(2)} (\mu_{\text{L}} (k_{a \to b}^{\text{L}} + k_{b \to a}^{\text{L}}) \\ &+ \mu_{\text{R}} (k_{a \to b}^{\text{R}} + k_{b \to a}^{\text{R}})) \end{split} \tag{44}$$

Using eqs 42 and 44, we can present the work—energy balance equation at this order as follows:

$$\dot{E}_{\rm M}^{(2)} = \dot{W}^{(2)} - J_{\rm tot}^{(2)} + (\mu_{\rm L} I_{\rm L}^{(2)} + \mu_{\rm R} I_{\rm R}^{(2)}) \tag{45}$$

where

$$\begin{split} \dot{E}_{M}^{(2)} &= -\frac{\mathrm{d}}{\mathrm{d}t} [\epsilon_{\mathrm{d}} G^{(1)}] \\ &= -\dot{\epsilon}_{\mathrm{d}}^{2} \left[\frac{\partial P_{a}^{0}}{\partial \epsilon_{\mathrm{d}}} \frac{1}{k_{a \to b} + k_{b \to a}} + \epsilon_{\mathrm{d}} \frac{d}{d\epsilon_{\mathrm{d}}} \left(\frac{\partial P_{a}^{0}}{\partial \epsilon_{\mathrm{d}}} \frac{1}{k_{a \to b} + k_{b \to a}} \right) \right] \end{split}$$

$$(46)$$

is the second order change rate in the total system energy expressed as the time derivative of the first order contribution to this energy (product of $\epsilon_{\rm d}$ and the first order correction to the population $G^{(1)}$) and

$$\dot{W}^{(2)} = -\dot{\epsilon}_{d} G^{(1)} \equiv -\dot{\epsilon}_{d}^{2} \frac{\partial P_{a}^{0}}{\partial \epsilon_{d}} \frac{1}{k_{a \to b} + k_{b \to a}}$$
(47)

is the second order excess work per unit time (power) which corresponds to the lowest order *irreversible* work expressing

dissipation caused by driving the level. The last term on the right-hand side of eq 45 represents the second order contribution to the rate of chemical work; thus, eq 45 is an expression for the first law of thermodynamics at the second order of our expansion. Following refs 68 and 86, the coefficient in front of $\dot{\varepsilon}_d^2$ in eq 45

$$\gamma = -\frac{\partial P_a^0}{\partial \epsilon_d} \frac{1}{k_{a \to b} + k_{b \to a}} \tag{48}$$

may be identified with the friction coefficient. A similar interpretation was suggested for different models for SMJs. 68,87

Dependencies of γ on ϵ_d are shown in Figure 3. In an unbiased junction the friction coefficient reaches its maximum

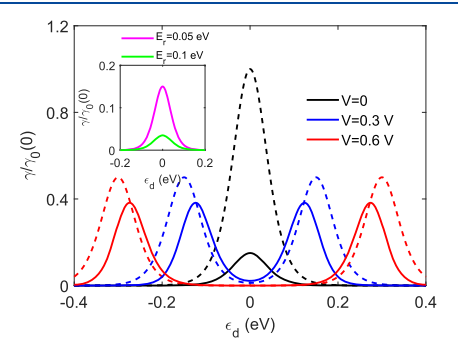


Figure 3. Friction coefficient characterizing dissipation in the system caused by driving of the energy level in a symmetrically coupled junction with a symmetrically applied bias as a function of $\epsilon_{\rm d}$. Main figure: Dashed lines represent friction in the absence of molecule-solvent coupling $(E_{\rm r}=0)$; solid lines are plotted at $E_{\rm r}=0.05$ eV for three values of the bias voltage (indicated by different colors). Inset: Friction at zero bias for the indicated two values of reorganization energy. In all lines, the friction is normalized by its value at zero bias and zero reorganization energy. Other parameters are $kT_{\rm L}=kT_{\rm R}=kT_{\rm s}=0.026$ eV, and $\hbar\Gamma=0.01$ eV. $\gamma_0(0)$ is the maximum value of the friction coefficient in the junction where the molecule is detached from the solvent $(E_{\rm r}=0)$.

 $\gamma(0)$ at $\epsilon_{\rm d}=\mu=0$ and falls approaching zero as $\epsilon_{\rm d}$ moves away from this position. In this case, γ appears to increase with the increasing voltage. This results from the fact that at low bias the Franck–Condon blockade discussed above makes the molecule–electrode coupling small, and the friction increases upon removing this blockade at higher bias voltage. Also, at higher voltage the peak splits: Two peaks appear due to electron–electrode exchange near the two Fermi energies characterizing the biased junction. Note that coupling to the solvent shifts the positions of these peaks, in correspondence with the eqs 5 and 6 for transfer rates.

III.C. Evolution of the System (Dot) Entropy. Define the system entropy by the Gibbs formula for our binary system

$$S = -k(P_a \ln P_a + (1 - P_a) \ln(1 - P_a))$$
(49)

Using eqs 28, we find

$$S = -k((P_a^0 - G)\ln(P_a^0 - G) + (1 - P_a^0 + G)\ln(1 - P_a^0 + G))$$
(50)

which can be used to find again an expansion in powers of $\dot{\varepsilon}_{\rm d}$: $S^{(0)} + S^{(1)} + ...$ In what follows we limit ourselves to the case of an unbiased junction in the wide-band limit for which $P_a^0/P_b^0 = \exp(-\beta \varepsilon_{\rm d})$. In the absence of driving

$$S^{(0)} = -k(P_a^{(0)} \ln P_a^{(0)} + (1 - P_a^{(0)}) \ln(1 - P_a^{(0)}))$$
 (51)

and (assuming that $T_L = T_R = T_s \equiv T$)

$$S^{(1)} = -k\beta \epsilon_{\mathbf{d}} G^{(1)} \tag{52}$$

The first and second order variations in the dot's entropy due to driving are obtained as (recall that the sign of J_{tot} was chosen so that the heat current into the environment is positive)

$$\dot{S}^{(1)} = \dot{\epsilon}_{\mathbf{d}} \frac{\partial S^{(0)}}{\partial \epsilon_{\mathbf{d}}} = \frac{1}{T} \epsilon_{\mathbf{d}} \dot{\epsilon}_{\mathbf{d}} \frac{\partial P_a^{(0)}}{\partial \epsilon_{\mathbf{d}}} = -\frac{J_{\text{tot}}^{(1)}}{T}$$
(53)

and

$$\dot{S}^{(2)} = \dot{\epsilon}_{d} \frac{\partial S^{(1)}}{\partial \epsilon_{d}} = -k\beta \dot{\epsilon}_{d} G^{(1)} - k\beta \epsilon_{d} \dot{\epsilon}_{d} \frac{\partial G^{(1)}}{\partial \epsilon_{d}}$$

$$= \frac{\dot{W}^{(2)}}{T} - \frac{J^{(2)}}{T} \tag{54}$$

Equation 54 may be rewritten as

$$\dot{S}^{(2)} + \frac{J^{(2)}}{T} = \frac{\dot{W}^{(2)}}{T} \tag{55}$$

The left side of eq 55 is the sum of the rate of total entropy change in the system (dot/molecule) $\dot{S}^{(2)}$ and the entropy flux into the electrodes and solvent environment. Together these terms give the total entropy production due to the irreversible nature of the process at this order. This result is identical to that obtained in fully quantum mechanical treatments of similar processes evaluated in the absence of coupling to solvent, 67,78,80 except for a sign difference in the heat definition. Here, the heat which is going *out* of the system is defined as positive.

IV. MARCUS JUNCTION ENGINE

In this section, we extend the above analysis to discuss a simple model that simulates an atomic scale engine. This can be achieved by imposing asymmetry on the coupling of the molecular bridge to the electrodes that enables to convert the motion of $\epsilon_{\rm d}$ to electron current between the electrodes. A simple choice is

$$\Gamma_{L}(\epsilon) = \Gamma \frac{\delta^{2}}{(\epsilon + \epsilon_{0})^{2} + \delta^{2}}$$

$$\Gamma_{R}(\epsilon) = \Gamma \frac{\delta^{2}}{(\epsilon - \epsilon_{0})^{2} + \delta^{2}}$$
(56)

This represents a situation where the moving level is coupled to wide-band electrodes via single-level gateway sites with energies \pm ϵ_0 attached to the left/right electrode. The parameter δ characterizes widths of the density of states peaks associated with these states. The electron transfer rates are calculated from eqs 5 and 6. In further calculations we assume that $\epsilon_{\rm d}$ varies according to

$$\epsilon_{\rm d}(t) = E_0 - E_1 \cos(2\pi t/\tau) \tag{57}$$

It is intuitively obvious that driving fast enough (small τ) to induce deviation of the dot population from instantaneous equilibrium with a choice of origin E_0 and amplitude E_1 that encompass the interval $(-\epsilon_0, \epsilon_0)$ will produce current from the

left to the right electrode which may be appreciable if ϵ_0 is sufficiently larger than $kT_{\rm L}=kT_{\rm R}=kT_{\rm s}\equiv kT$. Mathematically, we treat this deviation from equilibrium dot population (eq 59 and beyond) using our expansions in powers of $\dot{\epsilon}_{\rm d}$ for the relevant quantities. The current is given by the average over a period

$$\left\langle I \right\rangle_{\tau} = \frac{1}{\tau} \int_0^{\tau} dt \ I_{\rm L}(t) = \frac{1}{\tau} \int_0^{\tau} dt \ I_{\rm R}(t)$$
 (58)

where $I_K(t)$ values are given by eq 32. Further analytical progress can be made by expanding I_K in powers of $\dot{\epsilon}_d$. However, using this expansion implies that δ in eq 56 is large enough for the inequality $kT\Gamma(\epsilon) \gg \dot{\epsilon}_d$ to be satisfied for all ϵ . The lowest nonvanishing contribution to eq 58 is then

$$\left\langle I \right\rangle_{\tau}^{(2)} = \frac{1}{\tau} \int_{0}^{\tau} dt \ I_{L}^{(2)}(t) = \frac{1}{\tau} \int_{0}^{\tau} dt \ I_{R}^{(2)}(t)$$
 (59)

where the second order contributions to the currents are given by eq 43. Note that this is the excess current produced by driving which persists also in the absence of imposed bias. When a voltage bias is imposed so as to drive a current in the opposite direction to $\langle I \rangle_{\tau}^{(2)}$, the total current

$$\left\langle I\right\rangle_{\tau}(V) = I_{\rm ss}(V) + \left\langle I\right\rangle_{\tau}^{(2)}(V)$$
 (60)

can be used to define the power produced by the engine

$$\Pi(V) = V(I_{ss}(V) + \left\langle I \right\rangle_{\tau}^{(2)}(V)) \tag{61}$$

The device efficiency is defined as the ratio

$$\eta(V) = \frac{\Pi(V)}{\frac{1}{\tau} \int_0^{\tau} dt \ \dot{W}^{(2)}(V, t)}$$
(62)

Figure 4 shows the voltage dependence of these engine characteristics. Obviously, both vanish in the absence of load

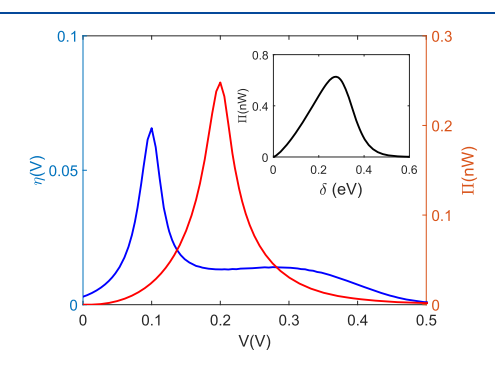


Figure 4. Averaged over the period thermodynamic efficiency η (blue line) and power Π (red line) produced in the junction by periodically driving the bridge level. Curves are plotted at kT=0.026 eV, $\hbar\Gamma=0.01$ eV, $E_0=0$, $E_1=0.1$ eV, $E_1=0.1$ eV, $E_0=0.1$ eV, $E_1=0.1$ e

(V=0), as well as at the stopping voltage when the current vanishes, and go through their maxima at different "optimal" voltages (which in turns depend on the choices of E_0 and E_1). Note that because of the intrinsic friction in this model, the efficiency vanishes rather than maximizes at the stopping

voltage point. The device operation depends on the characteristics of the molecule—metal coupling, expressed in our model by the parameters Γ , δ , and ϵ_0 . An example is shown in the inset to Figure 4. The produced power vanishes as the molecule—metal coupling goes to zero (a slip situation). It also vanishes for large δ , namely, when the coupling asymmetry disappears as $\Gamma(\epsilon)$ becomes independent of ϵ .

The definition of efficiency, eq 62, as the ratio between the generated power and the invested work, is limited to the regime where V is smaller than the stopping voltage and the current flows against the voltage bias. For higher counter voltage, current will flow in the opposite direction, and the efficiency as defined will become negative. In fact, the pump operation described above changes into a possible motor operation that can translate into conversion of electrical bias into mechanical work if a proper load is put on the molecular carrier. ^{88,89} Note that the gain of the machine may be defined as the total amount of charge transferred against the bias, so that at stopping voltage the current $I_{\rm ss}$ disappears. Mathematically, this means that the term proportional to $I_{\rm ss}$ disappears from eq 61. Physically, this means that the power vanishes when we stop the leakage current.

V. CONCLUSIONS

In the present work we have analyzed the energy balance in single-molecule junctions characterized by strong electron—phonon interactions, modeled by a single-level molecule (dot) connecting free electron metal electrodes, where charge transfer kinetics is described by Marcus electron transfer theory. The standard steady state transport theory was extended to include also slow driving of the molecular level that may be achieved by employing a time dependent gate potential. A consistent description of the energetics of this process was developed leading to the following observations:

- (a) Accounting for the total energy and its heat, work, and chemical components shows that energy conservation (first law of thermodynamics) is satisfied by this model at all examined orders of driving.
- (b) Heat is obviously produced by moving charge across a potential bias. In addition, when charge transfer involves solvent reorganization, the current flowing in a biased junction can bring about heat transfer between the metal and the solvent environments and may even produce solvent cooling in some voltage ranges.
- (c) In the presence of solvent reorganization, the friction experienced by the driven coordinate $\epsilon_{\rm d}$ which expresses energy loss (heat production) due to the moleculemetal electron exchange is strongly affected by the presence of solvent reorganization.
- (d) Beyond the reversible (driving at vanishingly small rate) limit, entropy is produced and is determined, at least to the second order in the driving speed, by the excess work associated with the friction affected by the molecule coupling to the electrodes and solvent environments.

We have also used this model to study a molecular junction with a periodically modulated dot energy. We have considered a model engine in which such periodic driving with a properly chosen energy dependent molecule—electrode coupling can move charge against a voltage bias and calculated the power and efficiency of such a device. In the parameter range consistent with our mathematical modeling, useful work can be

produced only in the irreversible regime, and we could determine the points of optimal performance of such an engine with respect to power and efficiency.

While our calculations are based on Marcus electron transfer kinetics in which level broadening due to molecule—metal coupling is disregarded, we have shown that the extension to the more general kinetics suggested in ref 38 which (approximately) bridges between Marcus sequential hopping and Landauer cotunneling limit is possible.

Energy conversion on the nanoscale continues to be a focus of intense interest. The present calculation provides a first simple step in evaluating such phenomena in a system involving electron transport, electron—solvent interaction, and mechanical driving.

APPENDIX A

Here, we derive eq 20 for $\dot{Q}_{\rm e}^{\rm L}$. Starting from eq 15, we present $Q_{{\rm e},a\to b}^{\rm L}$ in the form

$$\begin{split} Q_{e,a \to b}^{L} &= \epsilon_{\rm d} - E_{\rm r} - \mu_{\rm L} \\ &+ \frac{\Gamma}{k_{a \to b}^{\rm L}} \sqrt{\frac{\beta_{\rm s}}{4\pi E_{\rm r}}} \int {\rm d}\epsilon [1 - f_{\rm L}(\beta_{\rm L}, \, \epsilon)] \\ &\times (\epsilon + E_{\rm r} - \epsilon_{\rm d}) {\rm exp} \bigg[- \frac{\beta_{\rm s}}{4E_{\rm r}} (E_{\rm r} - \epsilon_{\rm d} + \epsilon)^2 \bigg] \end{split} \tag{A.1}$$

Similarly

$$Q_{e,b\to a}^{L} = \mu_{L} - \epsilon_{d} - E_{r} + \frac{\Gamma}{k_{b\to a}^{L}} \sqrt{\frac{\beta_{s}}{4\pi E_{r}}} \int d\epsilon f_{L}(\beta_{L}, \epsilon)$$

$$\times (\epsilon_{d} + E_{r} - \epsilon) \exp\left[-\frac{\beta_{s}}{4E_{r}} (E_{r} + \epsilon_{d} - \epsilon)^{2}\right]$$
(A.2)

Integrating by parts, we obtain

$$Q_{e,a\to b}^{L} = \epsilon_{d} - E_{r} - \mu_{L} - \frac{\Gamma}{k_{a\to b}^{L}} \sqrt{\frac{E_{r}}{\pi \beta_{s}}}$$

$$\times \int d\epsilon \frac{\partial f_{L}(\beta_{L}, \epsilon)}{\partial \epsilon} \exp \left[-\frac{\beta_{s}}{4E_{r}} (E_{r} - \epsilon_{d} + \epsilon)^{2} \right]$$
(A.3)

and

$$Q_{e,b\to a}^{L} = \mu_{L} - \epsilon_{d} - E_{r} - \frac{\Gamma}{k_{b\to a}^{L}} \sqrt{\frac{E_{r}}{\pi \beta_{s}}} \times \int d\epsilon \frac{\partial f_{L}(\beta_{L}, \epsilon)}{\partial \epsilon} \exp \left[-\frac{\beta_{s}}{4E_{r}} (E_{r} + \epsilon_{d} - \epsilon)^{2} \right]$$
(A.4)

Substituting these expressions into eq 18, we get the expression for \dot{Q}_e^L given by eq 20. Expressions for \dot{Q}_e^R and \dot{Q}_e^R and \dot{Q}_e^R and \dot{Q}_e and \dot{Q}_e

AUTHOR INFORMATION

Corresponding Author

Abraham Nitzan – Department of Chemistry, University of Pennsylvania, Philadelphia, Pennsylvania 19104, United States; School of Chemistry, Tel Aviv University, Tel Aviv 6997801, Israel; o orcid.org/0000-0002-8431-0967; Email: anitzan@sas.upenn.edu

Author

Natalya A. Zimbovskaya — Department of Physics and Electronics, University of Puerto Rico—Humacao, Humacao, Puerto Rico 00791, United States

Complete contact information is available at: https://pubs.acs.org/10.1021/acs.jpcb.0c00059

Notes

The authors declare no competing financial interest.

ACKNOWLEDGMENTS

The present work was supported by the U.S. National Science Foundation (DMR-PREM 1523463). Also, the research of A.N. is supported by the Israel-U.S Binational Science Foundation, the German Research Foundation (DFG TH 820/11-1), the U.S National Science Foundation (Grant CHE1665291), and the University of Pennsylvania. N.A.Z. acknowledges support of the Sackler Visiting Professor Chair at Tel Aviv University, Israel.

REFERENCES

- (1) Nitzan, A.; Ratner, M. A. Electron transport in molecular wire junctions. *Science* **2003**, *300*, 1384–1389.
- (2) Agrait, N.; Yeati, A. L.; Van Ruitenbeek, J. M. Quantum properties of atomic-sized conductors. *Phys. Rep.* **2003**, *377*, 81–279.
- (3) Coropceanu, V.; Cornil, J.; da Silva Filho, D. A.; Olivier, Y.; Silbey, R.; Bredas, J.-L. Charge transport in organic semiconductors. *Chem. Rev.* **2007**, *107*, 926–952.
- (4) Cuevas, J. C.; Sheer, E. Molecular Electronics: An Introduction to Theory and Experiment; World Scientific: Singapore, 2010.
- (5) Venkataraman, L.; Klare, J. E.; Nuckolls, C.; Hybertsen, M. S.; Steigerwald, M. L. Dependence of single-molecule junction conductance on molecular conformation. *Nature* **2006**, 442, 904–907.
- (6) Li, X.; Hihath, J.; Chen, F.; Masuda, T.; Zang, L.; Tao, N. G. Thermally activated electron transport in single redox molecules. *J. Am. Chem. Soc.* **2007**, *129*, 11535–11542.
- (7) Li, C.; Mishchenko, A.; Li, Z.; Pobelov, I.; Wandlowski, Th.; Li, X. Q.; Wurthner, F.; Bagrets, A.; Evers, F. Electrochemical gate-controlled electron transport of redox-active single perylene bisimide molecular junctions. *J. Phys.: Condens. Matter* **2008**, *20*, 374122.
- (8) Li, Z.; Liu, Y.; Mertens, S. F. L.; Pobelov, I. V.; Wandlowski, Th. From redox gating to quantized charging. *J. Am. Chem. Soc.* **2010**, *132*, 8187–8193
- (9) Galperin, M.; Ratner, M. A.; Nitzan, A. Molecular transport junctions: vibrational effects. *J. Phys.: Condens. Matter* **2007**, *19*, 103201.
- (10) Dubi, Y.; Di Ventra, M. Heat flow and thermoelectricity in atomic and molecular junctions. *Rev. Mod. Phys.* **2011**, *83*, 131–154.
- (11) Zimbovskaya, N. A.; Pederson, M. R. Electron transport through molecular junctions. *Phys. Rep.* **2011**, *509*, 1–87.
- (12) Cizek, M.; Thoss, M.; Domcke, W. Theory of vibrationally inelastic electron transport through molecular bridges. *Phys. Rev. B: Condens. Matter Mater. Phys.* **2004**, *70*, 125406.
- (13) Ren, J.; Zhu, J.-X.; Gubernatis, J. E.; Wang, C.; Li, B. Thermoelectric transport with electron-phonon coupling and electron-electron interaction in molecular junctions. *Phys. Rev. B: Condens. Matter Mater. Phys.* **2012**, *85*, 155443.
- (14) Walczak, K. Thermoelectric properties of vibrating molecule asymmetrically connected to the electrodes. *Phys. B* **2007**, 392, 173–179.

- (15) Koch, T.; Loos, J.; Fehske, H. Thermoelectric effects in molecular quantum dots with contacts. *Phys. Rev. B: Condens. Matter Mater. Phys.* **2014**, *89*, 155133.
- (16) Zimbovskaya, N. A. The effect of dephasing on the thermoelectric efficiency of molecular junctions. *J. Phys.: Condens. Matter* **2014**, *26*, 275303.
- (17) Koch, J.; von Oppen, F. Franck-Condon blockade and giant Fano factors in transport through single molecules. *Phys. Rev. Lett.* **2005**, *94*, 206804.
- (18) Koch, J.; von Oppen, F.; Andreev, A. Theory of the Franck-Condon blockade regime. *Phys. Rev. B: Condens. Matter Mater. Phys.* **2006**, 74, 205438.
- (19) Hartle, R.; Thoss, M. Vibrational instabilities in resonant electron transport through single-molecule junctions. *Phys. Rev. B: Condens. Matter Mater. Phys.* **2011**, 83, 125419.
- (20) Hartle, R.; Thoss, M. Resonant electron transport in single-molecule junctions: Vibrational excitation, rectification, negative differential resistance, and local cooling. *Phys. Rev. B: Condens. Matter Mater. Phys.* **2011**, 83, 115414.
- (21) Galperin, M.; Ratner, M. A.; Nitzan, A. Hysteresis, switching, and negative differential resistance in molecular junctions. A polaron model. *Nano Lett.* **2005**, *5*, 125–130.
- (22) Zazunov, A.; Feinberg, D.; Martin, T. Phonon-mediated negative differential conductance in molecular quantum dots. *Phys. Rev. B: Condens. Matter Mater. Phys.* **2006**, 73, 115405.
- (23) Marcus, R. A. On the Theory of Oxidation-Reduction Reactions Involving Electron Transfer. I. *J. Chem. Phys.* **1956**, 24, 966–982.
- (24) Marcus, R. A. Chemical and Electrochemical Electron-Transfer Theory. *Annu. Rev. Phys. Chem.* **1964**, *15*, 155–196.
- (25) Marcus, R. A.; Sutin, N. Electron transfers in chemistry and biology. *Biochim. Biophys. Acta, Rev. Bioenerg.* 1985, 811, 265-308.
- (26) Marcus, R. A. Electron transfer reactions in chemistry. Theory and experiment. *Rev. Mod. Phys.* **1993**, *65*, 599–653.
- (27) Nitzan, A. Chemical Dynamics in Condensed Phases: Relaxation, Transfer and Reactions in Condensed Molecular Systems; Oxford University Press, 2006.
- (28) Jia, C.; Migliore, A.; Xin, N.; Huang, S.; Wang, J.; Yang, Q.; Wang, S.; Chen, H.; Wang, D.; Feng, B.; Liu, Z.; Zhang, G.; Qu, D. H.; Tian, H.; Ratner, M. A.; Xu, H. Q.; Nitzan, A.; Guo, X. Covalently bonded single-molecule junctions with stable and reversible photoswitched conductivity. *Science* **2016**, *352*, 1443–1445.
- (29) Migliore, A.; Nitzan, A. Irreversibility and hysteresis in redox molecular conduction junctions. *J. Am. Chem. Soc.* **2013**, *135*, 9420–9432.
- (30) Migliore, A.; Schiff, P.; Nitzan, A. On the relationship between molecular state and single electron pictures in simple electrochemical junctions. *Phys. Chem. Chem. Phys.* **2012**, *14*, 13746.
- (31) Kuznetsov, A. M.; Medvedev, I. G. Coulomb repulsion effect on the tunnel current through the redox molecule in the weak tunneling limit. *Phys. Rev. B: Condens. Matter Mater. Phys.* **2008**, 78, 153403.
- (32) Kuznetsov, A. M.; Medvedev, I. G.; Ulstrup, J. Coulomb repulsion effect in two-electron nonadiabatic tunneling through a one-level redox molecule. *J. Chem. Phys.* **2009**, *131*, 164703.
- (33) Yuan, L.; Wang, L.; Garrigues, A. R.; Jiang, L.; Annadata, H. V.; Antonana, M. A.; Barco, E.; Nijhuis, C. A. Transition from direct to inverted charge transport Marcus regions in molecular junctions via molecular orbital gating. *Nat. Nanotechnol.* **2018**, *13*, 322–329.
- (34) Bueno, P. R.; Benites, T. A.; Davis, J. J. The mesoscopic electrochemistry of molecular junctions. Sci. Rep. 2016, 6, 18400.
- (35) Migliore, A.; Nitzan, A. Nonlinear charge transport in redox molecular junctions: A Marcus perspective. *ACS Nano* **2011**, *5*, 6669–6685.
- (36) Craven, G. T.; Nitzan, A. Electron transfer through a thermal gradient. *Proc. Natl. Acad. Sci. U. S. A.* **2016**, *113*, 9421–9432.
- (37) Craven, G. T.; Nitzan, A. Electron transfer at thermally heterogeneous molecule-metal interfaces. *J. Chem. Phys.* **2017**, *146*, 092305.

- (38) Sowa, J. K.; Mol, J. A.; Briggs, D.; Gauger, E. M. Beyond Marcus theory and the Landauer-Büttiker approach in molecular junctions: A unified framework. *J. Chem. Phys.* **2018**, *149*, 154112.
- (39) Sowa, J. K.; Lambert, N.; Seideman, T.; Gauger, E. M. Beyond Marcus theory and the Landauer-Buttiker approach in molecular junctions II. A self-consistent Born approach. *J. Chem. Phys.* **2020**, *152*, 064103.
- (40) Cahill, D. G.; Ford, W. K.; Goodson, K.; Mahan, G. D.; Majumdar, A.; Maris, H. J.; Merlin, R.; Phillpot, S. R. Nanoscale thermal transport. *J. Appl. Phys.* **2003**, *93*, 793–818.
- (41) Leitner, D. M. Thermal boundary conductance and thermal rectification in molecules. *J. Phys. Chem. B* 2013, 117, 12820–12828.
- (42) Leitner, D. M. Quantum ergodicity and energy flow in molecules. *Adv. Phys.* **2015**, *64*, 445–517.
- (43) Li, N.; Ren, J.; Wang, L.; Zhang, G.; Hanggi, P.; Li, B. Phononics: Manipulating heat flow with electronic analogs and beyond. *Rev. Mod. Phys.* **2012**, *84*, 1045–1089.
- (44) Luo, T.; Chen, G. Nanoscale heat transfer from computation to experiment. *Phys. Chem. Chem. Phys.* **2013**, *15*, 3389–3397.
- (45) Rubtsova, N. I.; Nyby, C. M.; Zhang, H.; Zhang, B.; Zhou, X.; Jayawickramarajah, J.; Burin, A. L.; Rubtsov, I. V. Room-temperature ballistic energy transport in molecules with repeating units. *J. Chem. Phys.* **2015**, *142*, 212412.
- (46) Marconnet, A. M.; Panzer, M. A.; Goodson, K. E. Thermal conduction phenomena in carbon nanotubes and related nanostructured materials. *Rev. Mod. Phys.* **2013**, *85*, 1295–1343.
- (47) Al-Ghalith, J.; Ni, Y.; Dumitrica, T. Nanowires with dislocations for ultralow lattice thermal conductivity. *Phys. Chem. Chem. Phys.* **2016**, *18*, 9888.
- (48) Foti, G.; Vazquez, H. Adsorbate-driven cooling of carbenebased molecular junctions. *Beilstein J. Nanotechnol.* **2017**, *8*, 2060–2068.
- (49) Chen, Y.-C.; Zwolak, M.; Di Ventra, M. Inelastic effects on the transport properties of alkanethiols. *Nano Lett.* **2005**, *5*, 621–624.
- (50) Losego, M. D.; Grady, M. E.; Sottos, N. R.; Cahill, D. G.; Braun, P. V. Effects of chemical bonding on heat transport across interfaces. *Nat. Mater.* **2012**, *11*, 502–506.
- (51) O'Brien, P. J.; Shenogin, S.; Liu, J. P.; Chow, K.; Laurencin, D.; Mutin, P. H.; Yamaguchi, M.; Keblinski, P.; Ramanath, G. Bonding-induced thermal conductance enhancement at inorganic heterointerfaces using nanomolecular monolayers. *Nat. Mater.* **2013**, *12*, 118–122.
- (52) Foti, G.; Vazquez, H. Interface tuning of current-induced cooling in molecular circuits. *J. Phys. Chem. C* **2017**, *121*, 1082–1088.
- (53) Segal, D. Thermoelectric effect in molecular junctions: A tool for revealing transport mechanisms. *Phys. Rev. B: Condens. Matter Mater. Phys.* **2005**, 72, 165426.
- (54) Wu, G.; Li, B. Thermal rectification in carbon nanotube intramolecular junctions: Molecular dynamics calculations. *Phys. Rev. B: Condens. Matter Mater. Phys.* **2007**, *76*, 085424.
- (55) Wu, L.-A.; Segal, D. Sufficient conditions for thermal rectification in hybrid quantum structures. *Phys. Rev. Lett.* **2009**, 102, 095503.
- (56) Lu, J.-T.; Zhou, H.; Jiang, J.-W.; Wang, J.-S. Phonon thermal transport in silicon-based nanomaterials. *AIP Adv.* **2015**, *5*, 053204.
- (57) Pecchia, A.; Romano, G.; Di Carlo, A. Theory of heat dissipation in molecular electronics. *Phys. Rev. B: Condens. Matter Mater. Phys.* **2007**, *75*, 035401.
- (58) Yang, N.; Xu, X.; Zhang, G.; Li, B. Thermal transport in nanostructures. AIP Adv. 2012, 2, 041410.
- (59) Galperin, M.; Saito, K.; Balatsky, A. V.; Nitzan, A. Cooling mechanisms in molecular conduction junctions. *Phys. Rev. B: Condens. Matter Mater. Phys.* **2009**, *80*, 115427.
- (60) Lykkebo, J.; Romano, G.; Gagliardi, A.; Pecchia, A.; Solomon, G. C. Single-molecule electronics: cooling Individual vibrational modes by the tunneling Current. J. Chem. Phys. 2016, 144, 114310.
- (61) Kilgour, M.; Segal, D. Coherence and decoherence in quantum absorption refrigerators. *Phys. Rev. E: Stat. Phys., Plasmas, Fluids, Relat. Interdiscip. Top.* **2018**, 98, 012117.

- (62) Marcus, R. A. On the theory of electron-transfer reactions. VI. Unified treatment for homogeneous and electrode reactions. *J. Chem. Phys.* **1965**, *43*, 679–694.
- (63) Stahler, J.; Meyer, M.; Zhu, X. Y.; Bovensiepen, U.; Wolf, M. Dynamics of electron transfer at polar molecule-metal interfaces: the role of thermally activated tunnelling. *New J. Phys.* **2007**, *9*, 394.
- (64) Zanetti-Polzi, L.; Corni, S. A dynamical approach to non-adiabatic electron transfers at the bio-inorganic interface. *Phys. Chem. Phys.* **2016**, *18*, 10538.
- (65) Zotti, L. A.; Burkle, M.; Pauly, F.; Lee, W.; Kim, K.; Jeong, W.; Asai, Y.; Reddy, P.; Cuevas, J. C. Heat dissipation and its relation to thermopower in single-molecule junctions. *New J. Phys.* **2014**, *16*, 015004.
- (66) This happens because the distribution of holes (empty electron states) below the Fermi energy μ and the distribution of electrons (occupied states) above the latter are the same. Both electrons and holes are coupled to the electrodes through the dot level. Therefore, at $\epsilon_{\rm d} = \mu$, the distributions of electrons and holes are symmetric, and the electron current cancels the hole current.
- (67) Lee, W.; Kim, K.; Jeong, W.; Zotti, L. A.; Pauly, F.; Cuevas, J. C.; Reddy, P. Heat dissipation in atomic-scale junctions. *Nature* **2013**, 498, 209–212.
- (68) Bruch, A.; Thomas, M.; Kusminskiy, S. V.; von Oppen, F.; Nitzan, A. Quantum thermodynamics of the driven resonant level model. *Phys. Rev. B: Condens. Matter Mater. Phys.* **2016**, 93, 115318.
- (69) Esposito, M.; Ochoa, M. A.; Galperin, M. Quantum Thermodynamics: A Nonequilibrium Green's Function Approach. *Phys. Rev. Lett.* **2015**, *114*, 080602.
- (70) Esposito, M.; Ochoa, M. A.; Galperin, M. Nature of heat in strongly coupled open quantum systems. *Phys. Rev. B: Condens. Matter Mater. Phys.* **2015**, 92, 235440.
- (71) Ludovico, M. F.; Arrachea, L.; Moskalets, M.; Sanchez, D. Probing the energy reactance with adiabatically driven quantum dots. *Phys. Rev. B: Condens. Matter Mater. Phys.* **2018**, *97*, 041416.
- (72) Ludovico, M. F.; Moskalets, M.; Sanchez, D.; Arrachea, L. Dynamics of energy transport and entropy production in ac-driven quantum electron systems. *Phys. Rev. B: Condens. Matter Mater. Phys.* **2016**, *94*, 035436.
- (73) Ludovico, M. F.; Battista, F.; von Oppen, F.; Arrachea, L. Adiabatic response and quantum thermoelectrics for ac-driven quantum systems. *Phys. Rev. B: Condens. Matter Mater. Phys.* **2016**, 93, 075136.
- (74) Ludovico, M. F.; Arrachea, L.; Moskalets, M.; Sanchez, D. Periodic energy transport and entropy production in quantum electronics. *Entropy* **2016**, *18*, 00419.
- (75) Ludovico, M. F.; Lim, J. S.; Moskalets, M.; Arrachea, L.; Sanchez, D. Dynamical energy transfer in ac-driven quantum systems. *Phys. Rev. B: Condens. Matter Mater. Phys.* **2014**, 89, 161306.
- (76) Thingna, J.; Barra, F.; Esposito, M. Kinetics and thermodynamics of a driven open quantum system. *Phys. Rev. E: Stat. Phys., Plasmas, Fluids, Relat. Interdiscip. Top.* **2017**, *96*, 052132.
- (77) Haughian, P.; Esposito, M.; Schmidt, T. L. Quantum thermodynamics of the resonant-level model with driven systembath coupling. *Phys. Rev. B: Condens. Matter Mater. Phys.* **2018**, 97, 085435.
- (78) Cavina, V.; Mari, A.; Giovannetti, V. Slow Dynamics and Thermodynamics of Open Quantum Systems. *Phys. Rev. Lett.* **2017**, 119, 050601.
- (79) Dou, W.; Ochoa, M. A.; Nitzan, A.; Subotnik, J. E. Universal approach to quantum thermodynamics in the strong coupling regime. *Phys. Rev. B: Condens. Matter Mater. Phys.* **2018**, 98, 134306.
- (80) Ochoa, M. A.; Bruch, A.; Nitzan, A. Energy distribution and local fluctuations in strongly coupled open quantum systems: The extended resonant level model. *Phys. Rev. B: Condens. Matter Mater. Phys.* **2016**, *94*, 035420.
- (81) Bruch, A.; Lewenkopf, C.; von Oppen, F. Landauer-Büttiker approach to strongly coupled quantum thermodynamics: Insideoutside duality of entropy evolution. *Phys. Rev. Lett.* **2018**, *120*, 107701.

- (82) Semenov, A.; Nitzan, A. Transport and thermodynamics in quantum junctions: A scattering approach. *arXiv* 2019, 1912.03773.
- (83) Migliore, A.; Nitzan, A. Irreversibility in redox molecular conduction: single versus double metal-molecule interfaces. *Electro-chim. Acta* **2015**, *160*, 363–375.
- (84) Oz, A.; Hod, A.; Nitzan, A. Numerical approach to nonequilibrium quantum thermodynamics: Nonperturbative treatment of driven resonant level model based on the driven Liouville von Neimann formalism. *J. Chem. Theory Comput.* **2020**, *16*, 1232.
- (85) The smallness of $\hat{\mathbf{e}}_{\mathrm{d}}$ should be established by comparison to $kT\Gamma$ and Γ^2/\hbar (ref 67).
- (86) Bode, N.; Kusminskiy, S. V.; Egger, R.; von Oppen, F. Current-induced forces in mesoscopic systems: A scattering-matrix approach. *Beilstein J. Nanotechnol.* **2012**, *3*, 144–162.
- (87) Einax, M.; Solomon, G. C.; Dieterich, W.; Nitzan, A. Unidirectional hopping transport of interacting particles on a finite chain. *J. Chem. Phys.* **2010**, *133*, 054102.
- (88) Bustos-Marún, R. A.; Refael, G.; von Oppen, F. Adiabatic quantum motors. *Phys. Rev. Lett.* **2013**, *111*, 060802.
- (89) Fernández-Alcázar, L. J.; Pastawski, H. M.; Bustos-Marún, R. A. Nonequilibrium current-induced forces caused by quantum localization: Anderson adiabatic quantum motors. *Phys. Rev. B: Condens. Matter Mater. Phys.* **2019**, 99, 045403.